JOURNAL OF GEOPHYSICAL RESEARCH, VOL. 114, D07201, doi:10.1029/2008JD010502, 2009

Click Here for Full Article

On the representation of droplet coalescence and autoconversion: Evaluation using ambient cloud droplet size distributions

W. C. Hsieh,[1] H. Jonsson,[2] L.-P. Wang,[3] G. Buzorius,[4] R. C. Flagan,[5,6] J. H. Seinfeld,[5,6] and A. Nenes[1,7]

Received 27 May 2008; revised 3 December 2008; accepted 30 January 2009; published 1 April 2009.

[1] In this study, we evaluate eight autoconversion parameterizations against integration of the Kinetic Collection Equation (KCE) for cloud size distributions measured during the NASA CRYSTAL-FACE and CSTRIPE campaigns. KCE calculations are done using both the observed data and fits of these data to a gamma distribution function; it is found that the fitted distributions provide a good approximation for calculations of total coalescence but not for autoconversion because of fitting errors near the drop-drizzle separation size. Parameterizations that explicitly compute autoconversion tend to be in better agreement with KCE but are subject to substantial uncertainty, about an order of magnitude in autoconversion rate. Including turbulence effects on droplet collection increases autoconversion by a factor of 1.82 and 1.24 for CRYSTAL-FACE and CSTRIPE clouds, respectively; this enhancement never exceeds a factor of 3, even under the most aggressive collection conditions. Shifting the droplet-drizzle separation radius from 20 to 25 μm results in about a twofold uncertainty in autoconversion rate. The polynomial approximation to the gravitation collection kernel used to develop parameterizations provides computation of autoconversion that agree to within 30%. Collectively, these uncertainties have an important impact on autoconversion but are all within the factor of 10 uncertainty of autoconversion parameterizations. Incorporating KCE calculations in GCM simulations of aerosol-cloud interactions studies is computationally feasible by using precalculated collection kernel tables and can quantify the autoconversion uncertainty associated with application of parameterizations.

Citation: Hsieh, W. C., H. Jonsson, L.-P. Wang, G. Buzorius, R. C. Flagan, J. H. Seinfeld, and A. Nenes (2009), On the representation of droplet coalescence and autoconversion: Evaluation using ambient cloud droplet size distributions, *J. Geophys. Res.*, *114*, D07201, doi:10.1029/2008JD010502.

1. Introduction

[2] Quantifying the impacts of aerosol on global cloud, known as the ''aerosol indirect climatic effect'' is an important agent of climate change. Increases in aerosol concentration from natural background levels tend to decrease average cloud drop size, which enhances cloud albedo (''first indirect effect'' [*Twomey*, 1977]) and can reduce precipitation efficiency (''second indirect effect'' [*Albrecht*, 1989]). The precipitation rate predicted in general circulation models (GCMs) is controlled by autoconversion, the process of collision-coalescence that leads to the formation of new small drizzle drops; changes in precipitation from aerosol effects are then represented as changes in the autoconversion rate. Estimates of indirect effects are subject to large uncertainty [*Intergovernmental Panel on Climate Change* (*IPCC*), 2007], a result of the incomplete representation of cloud microphysical processes, especially autoconversion of cloud water to rain [*Lohmann and Feichter*, 2005, 1997; *Jones et al.*, 2001; *Menon et al.*, 2002, 2003]. Predicted spatial and temporal evolution of liquid water path (LWP) in large-scale models is strongly influenced by the autoconversion scheme; hence accurately quantifying the autoconversion rate is ultimately required for reducing indirect effect uncertainty.

[3] Drizzle drops, defined as those with radius larger than a threshold, r_0 (typically 20 μm with corresponding mass x_0 [*Wood and Blossey*, 2005]), are the precursor to rain and are produced mainly by the collisions of small cloud droplets from activation of Cloud Condensation Nuclei (CCN). ''Autoconversion'' can then be defined as the coalescence of cloud droplets, each with mass less than x_0, to form

[1] School of Earth and Atmospheric Sciences, Georgia Institute of Technology, Atlanta, Georgia, USA.
[2] Center for Interdisciplinary Remotely-Piloted Aircraft Studies, Marina, California, USA.
[3] Department of Mechanical Engineering, University of Delaware, Newark, Delaware, USA.
[4] Department of Meteorology, Graduate School of Engineering and Applied Sciences, Naval Postgraduate School, Monterey, California, USA.
[5] Environmental Science and Engineering, California Institute of Technology, Pasadena, California, USA.
[6] Department of Chemical Engineering, California Institute of Technology, Pasadena, California, USA.
[7] School of Chemical and Biomolecular Engineering, Georgia Institute of Technology, Atlanta, Georgia, USA.

Copyright 2009 by the American Geophysical Union.
0148-0227/09/2008JD010502$09.00

drizzle drops of mass larger than x_0. A collision event can also produce a cloud drop with mass less than x_0, and is called "self-collection" [*Beheng and Doms*, 1986; *Beheng*, 1994; *Seifert and Beheng*, 2001]. If the droplet size distribution is known, the autoconversion rate A can be computed from the Kinetic Collection Equation (KCE) [*Pruppacher and Klett*, 1997; *Wood and Blossey*, 2005]:

$$A = \int_0^{x_0} \left[\int_{x_0 - x}^{x_0} K(x, x') x' n(x') dx' \right] n(x) dx \tag{1}$$

where $K(x, x')$ is the collection kernel and $n(x)$ is the drop size distribution (DSD).

[4] Explicitly resolving the collection process is generally considered computationally expensive [*Khairoutdinov and Kogan*, 2000; *Randall et al.*, 2003] and has seen limited usage in GCM simulations. Instead, parameterizations are used, where the autoconversion rate is expressed in terms of size distribution moments, such as liquid water content (LWC) [*Kessler*, 1969], cloud droplet number concentration (CDNC) [*Manton and Cotton*, 1977; *Baker*, 1993; *Rotstayn*, 1997; *Khairoutdinov and Kogan*, 2000], and spectral dispersion [*Beheng*, 1994; *Cohard and Pinty*, 2000; *Liu and Daum*, 2004]. Parameterizations are often developed from simplified forms of KCE with prescribed cloud droplet size distributions and collection kernels. For example, *Manton and Cotton* [1977] developed a formulation assuming that autoconversion is a threshold process, which commences once a "critical" value for liquid water content is exceeded. When autoconversion is active, an average collision frequency is assumed for all cloud droplets, resulting in an autoconversion rate that scales with $\mathrm{LWC}^{7/3}$. *Liu and Daum* [2004] developed an analytical expression for autoconversion rate as a function of LWC, CDNC, and the relative dispersion (a measure of DSD width) of the cloud drop size distribution. Their formulation is derived by analytically integrating the KCE, using an approximate form of the gravitational collection kernel assuming the DSD follows a gamma distribution. The magnitude of autoconversion rate is given by the product of rate function and threshold function, as the later represents the fraction of the total coalescence and is recently derived as a function of droplet distribution width [*Liu et al.*, 2006]. Another approach to developing autoconversion parameterizations is to derive them from detailed microphysical simulations with a numerical cloud model. *Khairoutdinov and Kogan* [2000] adopted this approach, and used a wide range of simulated DSDs obtained from Large-Eddy Simulation (LES) of drizzling marine stratocumulus to fit autoconversion rates (using least squares minimization) to simple power law expressions that depend on droplet number and liquid water content.

[5] Autoconversion parameterizations are subject to considerable uncertainty, as when applied to the same cloud microphysical state can give autoconversion rates that vary up to three orders of magnitude [e.g., *Wood and Blossey*, 2005]. The implications are very important for hydrological cycle simulations, as the timescale for forming precipitation (especially in stratiform clouds) can be in substantial error, leading to systematic shifts in precipitation patterns. The process of "tuning" a parameterization to match observed precipitation patterns [e.g., *Rotstayn*, 1997] may partially offset this bias, but is inherently limited owing to the multiple scales involved and the nonlinearity of the autoconversion process.

[6] Many reasons exist for the large differences seen between autoconversion parameterizations. First, parameterizations do not necessarily use the same definition for autoconversion. For example, the threshold size used for separating drizzle from cloud drops by *Khairoutdinov and Kogan* [2000] is 25 μm, and, 20 μm by *Wood and Blossey* [2005]. *Liu and Daum* [2004] do not consider a threshold at all, and instead predict total coalescence P (i.e., all collection events, regardless of their droplet size), done by changing the integration limits of (1) to,

$$P = \int_0^{\infty} \left[\int_0^{\infty} K(x, x') x' n(x') dx' \right] n(x) dx \tag{2}$$

[7] Uncertainty in predicted autoconversion may also result from the DSD assumed (e.g., gamma or lognormal) in the development of each formulation. Substantial uncertainties in predictions of autoconversion rate also arise from the form of the collection kernel used. The essential kernel is that for gravitational coalescence under quiescent conditions, and is that which the exclusive majority of parameterizations employ. Cloud-scale turbulence however is known to augment the coalescence rate, and can be included by adding a turbulent kernel into the collection process [e.g., *Riemer and Wexler*, 2005; *Riemer et al.*, 2007]. Incorporating turbulence effects in a parameterization, however, is challenging, given the complex form of the collection kernel [e.g., *Ayala et al.*, 2008a, 2008b]. Whether or not turbulence effects should be included in parameterizations still remains an open question, given that the augmentation in autoconversion rate may still be within the inherent uncertainty of parameterizations.

[8] In this study, we assess the importance of assumptions used in the development of autoconversion parameterizations. We first examine the error in autoconversion associated with using an analytic distribution (such as the gamma distribution), by comparing predicted autoconversion rates from the KCE employing observed distributions and fits to them. KCE calculations of autoconversion rate are then compared against parameterizations, to characterize their inherent uncertainty. We also explore the sensitivity of predicted autoconversion to the droplet size threshold used for calculating A, by comparing KCE calculations of A against P. The importance of including turbulence effects in KCE calculations of autoconversion rate is also examined. Finally, we assess the computational efficiency of KCE against autoconversion parameterizations.

2. Cloud Microphysics

2.1. Observational Data Sets

[9] Cloud droplet size distributions used in this study were collected aboard the CIRPAS Twin Otter aircraft (http://www.cirpas.org/) during two field campaigns: CRYSTAL-FACE in Key West, FL (July 2002) and CSTRIPE in Monterey, CA (July 2003). Measurements taken during CRYSTAL-FACE focused on low-level cumuliform clouds [*Conant et al.*, 2004; *VanReken et al.*, 2003], whereas

Table 1. Droplet Size Distribution Characteristics of Clouds Sampled During CRYSTAL-FACE and CSTRIPE

Cloud Property	Mean Value	Standard Deviation	Percentile		
			25th	50th	75th
		CRYSTAL-FACE			
LWC (kg m^{-3})	4.80×10^{-4}	4.06×10^{-4}	1.80×10^{-4}	3.45×10^{-4}	6.98×10^{-4}
CDNC (cm^{-3})	480	367	227	365	593
$\overline{D_p}$ (μm)	10.67	4.00	7.78	9.67	13.67
σ_p (μm)	4.34	2.28	2.49	3.51	6.06
ε	0.41	0.10	0.34	0.41	0.47
		CSTRIPE			
LWC (kg m^{-3})	1.50×10^{-4}	9.56×10^{-5}	5.89×10^{-5}	1.39×10^{-4}	2.39×10^{-4}
CDNC (cm^{-3})	304	97	234	298	370
$\overline{D_p}$ (μm)	7.18	2.08	5.22	7.22	8.79
σ_p (μm)	3.84	0.89	3.29	3.74	4.64
ε	0.56	0.12	0.47	0.55	0.64

marine stratocumulus clouds were the focus of CSTRIPE [*Meskhidze et al.*, 2005]. Detailed description of flights and sampling strategies for both campaigns are provided in the study by *VanReken et al.* [2003], *Conant et al.* [2004], and *Meskhidze et al.* [2005]. In both campaigns, droplet size distributions were measured with a Cloud and Aerosol Spectrometer (CAS) optical probe [*Baumgardner et al.*, 2001] and a Forward Scattering Spectrometer Probe (FSSP) [*Brenguier et al.*, 1998]. The observed DSDs range between 1 to 25 μm in radius; haze droplets (less than 1 μm) and their impact on collection will not be considered. We use transect averages for KCE calculations (using higher resolution data does not affect the closure between parameterizations and KCE); 164 transects are available from CRYSTAL-FACE, and 52 from CSTRIPE. Table 1 summarizes DSD characteristics (LWC, CDNC, mean droplet diameter $\overline{D_p}$, standard deviation σ_p for $\overline{D_p}$, and relative dispersion ε) for CRYSTAL-FACE and CSTRIPE data. In CRYSTAL-FACE (CSTRIPE) clouds, 25th and 75th percentiles of CDNC are 227 (234) cm^{-3} and 593 (370) cm^{-3}. The 25th and 75th percentiles of mean diameter for CRYSTAL-FACE (CSTRIPE) are 7.78 (5.22) μm and 13.67 (8.79) μm. Compared to CRYSTAL-FACE, CSTRIPE clouds are characterized by smaller LWC, CDNC, $\overline{D_p}$ and σ_p; this is consistent with the weaker dynamics and cloud depths associated with marine stratocumulus.

2.2. Autoconversion Parameterizations Studied

[10] The parameterization schemes used in this study are summarized in Table 2 and include (1) MC [*Manton and Cotton*, 1977], (2) BH [*Beheng*, 1994], (3) KK [*Khairoutdinov and Kogan*, 2000], (4) LD4 [*Liu and Daum*, 2004], (5) LD6 [*Liu and Daum*, 2004], (6) SD-L for over land, and, SD-O for over ocean (by *Sundqvist et al.* [1989], with modifications by *Del Genio et al.* [1996] to include a stronger dependence of autoconversion on LWC). These parameterizations, when applied to the same cloud, predict substantially different autoconversion rates. Analogous to Figure 1 of *Wood* [2005], Figure 1 presents predicted autoconversion rate for each parameterization in Table 2. The assumed CDNC is 300 cm^{-3}, and the relative dispersion is taken as 0.5 for the LD4, LD6, and BH parameterizations. At these cloud conditions, the BH scheme exhibits the largest dynamic range of autoconversion rate. KK generally predicts the lowest autoconversion rate and LD4 the highest; the two expressions on average differ by a factor of 120, and at low values of LWC, by three orders of magnitude. At lower LWC range, SD-O is close to LD6, but for LWC $> \sim$1.3 g m^{-3} converges to SD-L. To assess the importance of these differences, one can express them in terms of a timescale for rain formation, τ_{rain}. Since autoconversion is the rate-limiting step for forming rain [*Cohard and Pinty*, 2000], τ_{rain} can be approximated with the timescale of autoconversion, $\tau_{\text{auto}} = \text{LWC}/A$. If, for example, a cloud is characterized by LWC $\sim$ 1 g m^{-3} and an autoconversion rate of $\sim 10^{-7}$ kg m^{-3} s^{-1}, $\tau_{rain} \sim 2.7$ h; hence, such a cloud may form rain during its lifetime (20 mins to few hours); for clouds with lower autoconversion rates ($<10^{-8}$), τ_{rain} is too large (>27 h), and such clouds are unlikely to produce rain. Hence a factor of 10 difference in autoconversion in the $\sim 10^{-8}$–10^{-7} range represents the difference between a precipitating and non-precipitating cloud. Large uncertainties in autoconversion rates when $A < 10^{-9}$ or $A > 10^{-6}$ are, on the other hand, less important.

3. Parameterizations Versus KCE With Fitted DSD

[11] In this section, we assess the ability of LD6 to reproduce the autoconversion and total mass collection rate predicted by integration of KCE for gamma distributions (obtained from fits to ambient observed size distributions). Other parameterizations are not evaluated here, since the fitted and observed DSD have identical microphysical moments (i.e., CDNC, LWC, ϵ); the comprehensive intercomparison will be considered in section 4. In the following sections, we present the procedure to fit a gamma distribution to observed DSDs, and then proceed to quantifying the error in autoconversion rate associated with (1) assuming $P = A$ and (2) using the polynomial approximation to the gravitational collection kernel as the former is used in the derivation of LD6.

3.1. Relating Gamma Distribution to DSD Moments

[12] A DSD is said to follow a gamma distribution, $n(r)$, with shape parameter k and scale parameter θ, if [*Liu and Daum*, 2004],

$$n(r) = N_0 r^{k-1} e^{-r/\theta} \tag{3}$$

N_0, k and θ are constants, and can be related to the total droplet number concentration N, the liquid water content

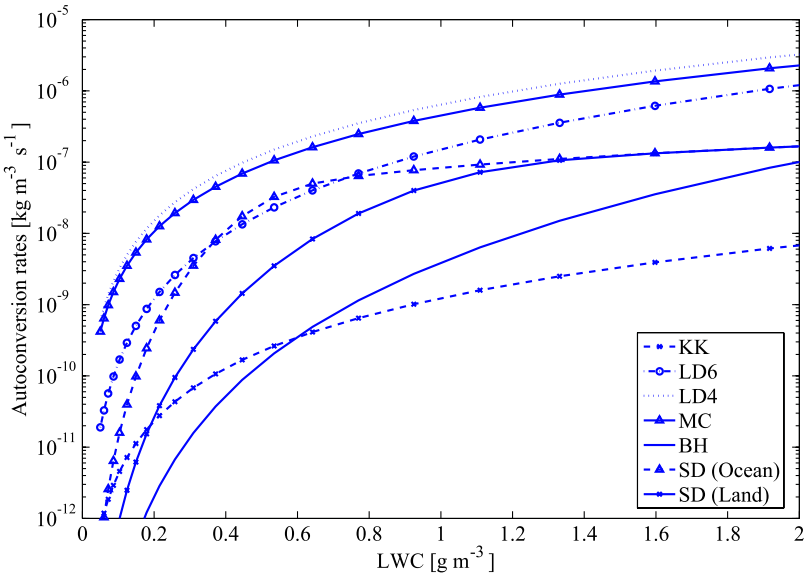

Figure 1. Autoconversion rate predicted by the parameterizations in Table 2, as a function of LWC for a cloud with a total drop concentration of 300 cm^{-3}. For LD4, LD6 and BH, a spectral dispersion of 0.5 is assumed.

LWC obtained from the measured distributions, and the relative dispersion ε (a measure of the width of $n(r)$),

$$\varepsilon = \sigma / r_m \tag{4}$$

where σ, r_m are the standard deviation and mean radius of the cloud drop distribution,

$$\sigma = \sqrt{\frac{\int_0^\infty (r - r_m)^2 n(r) dr}{\int_0^\infty n(r) dr}} \tag{5}$$

$$r_m = \frac{\int_0^\infty r n(r) dr}{\int_0^\infty n(r) dr} \tag{6}$$

[13] N_0 is expressed in terms of k and θ from the zeroth moment of measured DSD:

$$N_0 = \frac{N}{\Gamma(k)\theta^k} \tag{7}$$

where Γ is the gamma function and k is related to the observed relative dispersion, which is given by [*Liu and Daum*, 2004]:

$$k = \varepsilon^{-2} \tag{8}$$

[14] The parameter θ in equation (3) is determined by equating the third moment of the gamma distribution with the measured LWC [*Cohard and Pinty*, 2000],

$$\theta = \left(\frac{6}{\pi} \frac{LWC}{\rho_w} \frac{\Gamma(k)}{\Gamma(3+k)} \right)^{1/3} \tag{9}$$

3.2. Procedure for Fitting DSD and Calculation of A

[15] The gamma distribution fit to each measured DSD (equation (3)) is determined by first computing the LWC, σ_c, and r_m from the observed data. Then, k is computed from equations (4) and (8); θ is computed from equation (9), and N_0 from equation (7). Examples of measured vs. fitted distributions for the two field campaigns are given in Figure 2. In general, the gamma distribution provides a better fit to CRYSTAL-FACE data (which tend to be narrow) than for

Table 2. Autoconversion Parameterizations Considered in This Study[a]

Scheme	Autoconversion Rate (kg m^{-3} s^{-1})
MC [*Manton and Cotton*, 1977]	$A_{MC} = \pi\kappa_1 \left(\frac{3}{4\pi\rho_w}\right)^{4/3} E N^{-1/3} L^{7/3} H(R_3 - R_{3c})$
BH [*Beheng*, 1994]	$A_{BH} = -6.0 \times 10^{28}\, w^{-1.7} (N \times 10^{-6})^{-3.3} (L \times 10^{-3})^{4.7}$
KK [*Khairoutdinov and Kogan*, 2000]	$A_{KK} = 1350 q_c^{2.47} (N \times 10^{-6})^{-1.79}$
LD4 [*Liu and Daum*, 2004]	$P_{LD4} = \pi\kappa_1 \left(\frac{3}{4\pi\rho_w}\right)^{4/3} E \beta_4^4 N^{-1/3} L^{7/3} H(R_4 - R_{4c})$
LD6 [*Liu and Daum*, 2004]	$P_{LD6} = \left(\frac{3}{4\pi\rho_w}\right) \kappa_2 \beta_6^6 \left(\frac{L}{N}\right)^{2/3} N^{-1/3} L^{7/3} H(R_6 - R_{6c})$
SD [*Sundqvist et al.*, 1989]	$A_{SD} = C_0 q_c \left\{1 - \exp\left[-\left(\frac{L}{L_c}\right)^4\right]\right\}$

[a] L is liquid water content, N is the drop number concentration; the Stokes constant $k_1 = 1.19 \times 10^8$ m^{-1} s^{-1} and $k_2 = 1.9 \times 10^{17}$ m^{-3} s^{-1}. E is the average collection efficiency, taken as 0.55 [*Manton and Cotton*, 1977]. ρ_w is the density of water, and q_c is the cloud water mixing ratio. w is the width parameter related to the relative dispersion coefficient $\varepsilon = (w+1)^{-1/2}$. R_3, R_{3c}, R_4, R_{4c}, R_6, R_{6c} are mean and critical radius of third, fourth, sixth moments of droplet size distribution, respectively. β_4, β_6 are coefficients related to ϵ [*Liu and Daum*, 2004]. L_c is the critical cloud water content for the onset of rapid conversion (5×10^{-4} kg m^{-3} over land, 10^{-3} kg m^{-3} over ocean) and $C_0 = 10^{-4}$ s^{-1} is the limiting autoconversion rate.

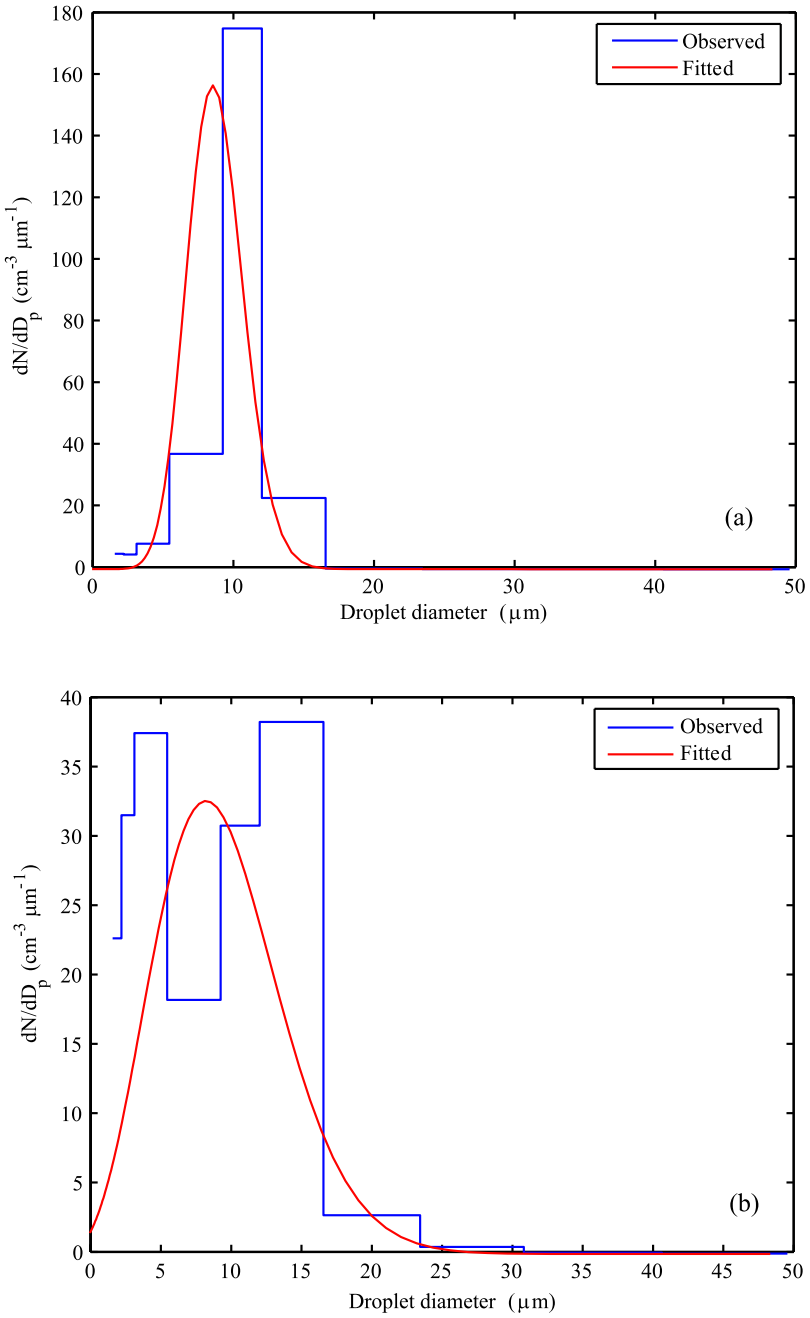

Figure 2. Examples of measured and fitted DSDs: (a) CRYSTAL-FACE C4 cloud (transect 3) and (b) CSTRIPE CS1 cloud (transect 4).

CSTRIPE; the importance of these discrepancies is assessed in section 3.3.

[16] After determining the k, θ and N_0 for each measured DSD, we proceed with computing A (equation (1)) for the fitted $n(r)$ of each measured distribution. This is done by discretizing $n(r)$ onto a grid; the number of droplets in each size bin is equal to $F(r_+) - F(r_-)$, where r_-, r_+ are the lower and upper size bounds of the discretized droplet bin, respectively, and $F(r)$ is the cumulative number concentration from 0 to r,

$$F(r) = \int_0^r N_0 \chi^{k-1} e^{-\chi/\theta} d\chi = N_0 \theta^k \gamma\left(k, \frac{r}{\theta}\right) \tag{10}$$

where γ is the incomplete gamma function [*Abramowitz and Stegun*, 1965].

[17] When computing A (equation (1)) or P (equation (2)), the polynomial approximation to the gravitational collection kernel (for $r \leq 50$ μm) is used [*Long*, 1974],

$$K(r_1, r_2) = K_2\left(r_1^6 + r_2^6\right) \tag{11}$$

with $K_2 = 0.04 \times 10^{15}$ m^{-3} s^{-1}; r_1 and r_2 are the colliding droplet radii (m). Equations (1) and (2) are then numerically integrated with the discretized size distributions to obtain the autoconversion rate. For measured DSDs, we use the CAS size bins (covering 1 to 25 μm in mean radius) and for

Table 3. The Mean Error and Standard Deviation of Total Coalescence and Autoconversion Rate From KCE Integration[a]

	$\log(A_{measured}/A_{fitted})$	
Data Set	Mean	Standard Deviation
Total Coalescence		
CRYSTAL-FACE	−0.01	0.13
CSTRIPE	0.33	0.29
Autoconversion Rate		
CRYSTAL-FACE	3.55	5.70
CSTRIPE	5.18	3.50

[a]Calculations are done using fitted and measured DSD for CRYSTAL-FACE and CSTRIPE data sets. The difference is represented in terms of orders of magnitude.

the fitted gamma distribution, we discretize over 100 sections with logarithmically spaced size bins from 1 to 25 μm in radius.

3.3. Appropriateness of Gamma Distribution Fits for Coalescence and Autoconversion

[18] The sensitivity of KCE integration to the specified DSD is evaluated first using the fitted DSDs for CRYSTAL-FACE clouds. The excellent agreement between LD6 and KCE (average relative difference, 5%) confirms that the polynomial collection kernel (used in the analytical derived LD6) is a good approximation to equation (11). Table 3 summarizes the mean error and standard deviation in predicted coalescence and autoconversion rates that results from fitting the observed CRYSTAL-FACE and CSTRIPE DSDs to a gamma function (section 3.2). Generally, the mean error for autoconversion that results by fitting distributions is much greater than for total coalescence; in fact, the total coalescence is well captured by the fit, even for the broad size distributions of CSTRIPE (which may not be described well by a gamma distribution, Figure 2b). This implies that the autoconversion computation by integrating KCE is very sensitive to the fitting distributions, because the distribution of droplets which are close to the drizzle threshold size strongly depends on the distribution function used. To estimate the autoconversion uncertainty resulting from the droplet binning scheme, the fitting procedure of size distribution is also repeated with designated particle bins from CAS probe. The difference in autoconversion is decreased but still large (2.66 for CRYSTAL-FACE, 4.17 for CSTRIPE). Most of this uncertainty arises from the deviations in the fitted distribution to the observations at large droplet sizes (which is more pronounced for the CSTRIPE data set); the latter effect is magnified when autoconversion is computed. This suggests that the skewness of DSD may need to be accounted for an effective parameterization of the autoconversion process.

4. Parameterizations Versus KCE With Measured DSD

[19] Here we quantify the autoconversion rate discrepancy between KCE calculations using the observed DSD and the parameterizations of Table 2. Figure 3 presents the predicted total coalescence of cloud droplets calculated using LD6, against KCE computations for observed CRYSTAL-FACE DSDs. The agreement between the total coalescence from KCE and LD6 is almost as close as in the evaluation using fitted (gamma function) DSDs (not shown). For higher autoconversion rates (10^{-7}–10^{-6}, which correspond to clouds most susceptible to rain formation), LD6 overestimates coalescence by about a factor of 2 (Figure 3); however, this may not be important for simulations of the hydrological cycle, as the precipitation timescale is already small for such clouds. This further supports that prescribing a gamma distribution is a good approximation for calculations of total coalescence.

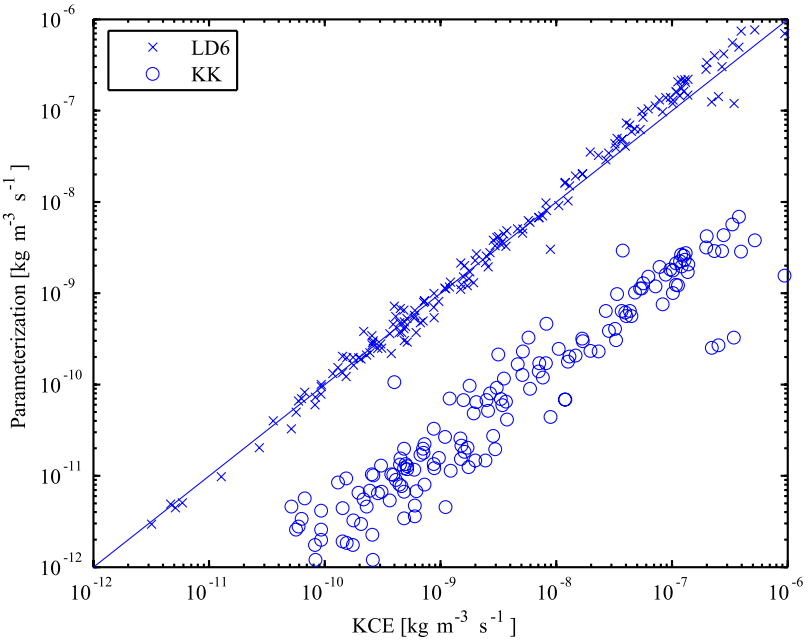

Figure 3. Parameterized autoconversion versus total coalescence from KCE calculations for measured CRYSTAL-FACE DSDs. Note that LD6 predicts total coalescence [*Wood and Blossey*, 2005].

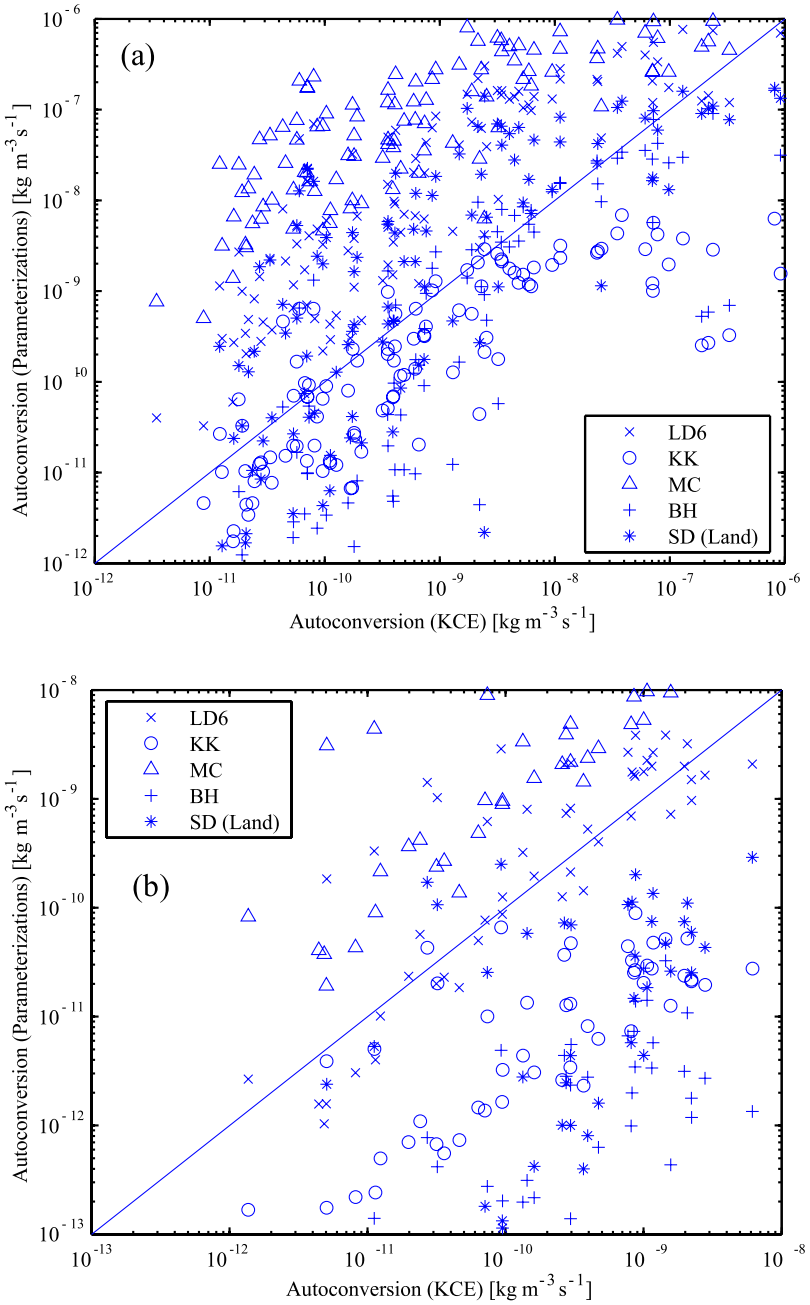

Figure 4. Autoconversion rates predicted by LD6, KK, MC, BH, and SD-L parameterizations versus KCE calculations using measured DSDs from (a) CRYSTAL-FACE and (b) CSTRIPE.

[20] Total coalescence is not autoconversion; because LD6 predicts total coalescence rate, it overestimates autoconversion by about a factor of 49 for CRYSTAL-FACE and 5 for CSTRIPE clouds (Figure 4). This is consistent with the study by *Wood and Blossey* [2005], who showed an overestimation by a factor of 3.8 to 112 for marine boundary layer clouds sampled in the northeast Atlantic Ocean. This overestimation does not exhibit a constant bias, nor does it have a strong correlation with LWC, given that the ratio of self-collection to autoconversion varies significantly between clouds (Figure 5a). However, the ratio correlates strongly with τ_{auto} (Figure 5b); application of LD6 would give a good approximation to A when the ratio is less than unity, i.e., only for heavily drizzling clouds with $\tau_{auto} < 30$ hr for CSTRIPE, and, $\tau_{auto} < 3$ hr for CRYSTAL-FACE (Figure 5b). The KK parameterization (which was explicitly developed to provide A) predicts systematically lower conversion when compared to LD6 (Figure 3). KK is in better agreement with KCE integrations for autoconversion rate (equation (1) for $r_0 = 20$ μm [*Wood and Blossey*, 2005]) and consistently tends to give the lowest mean error for CRYSTAL-FACE clouds (Table 4, Figure 4), but is still subject to substantial uncertainty (Figure 4; Table 4). As substantial as it may seem, this scatter is within the inherent

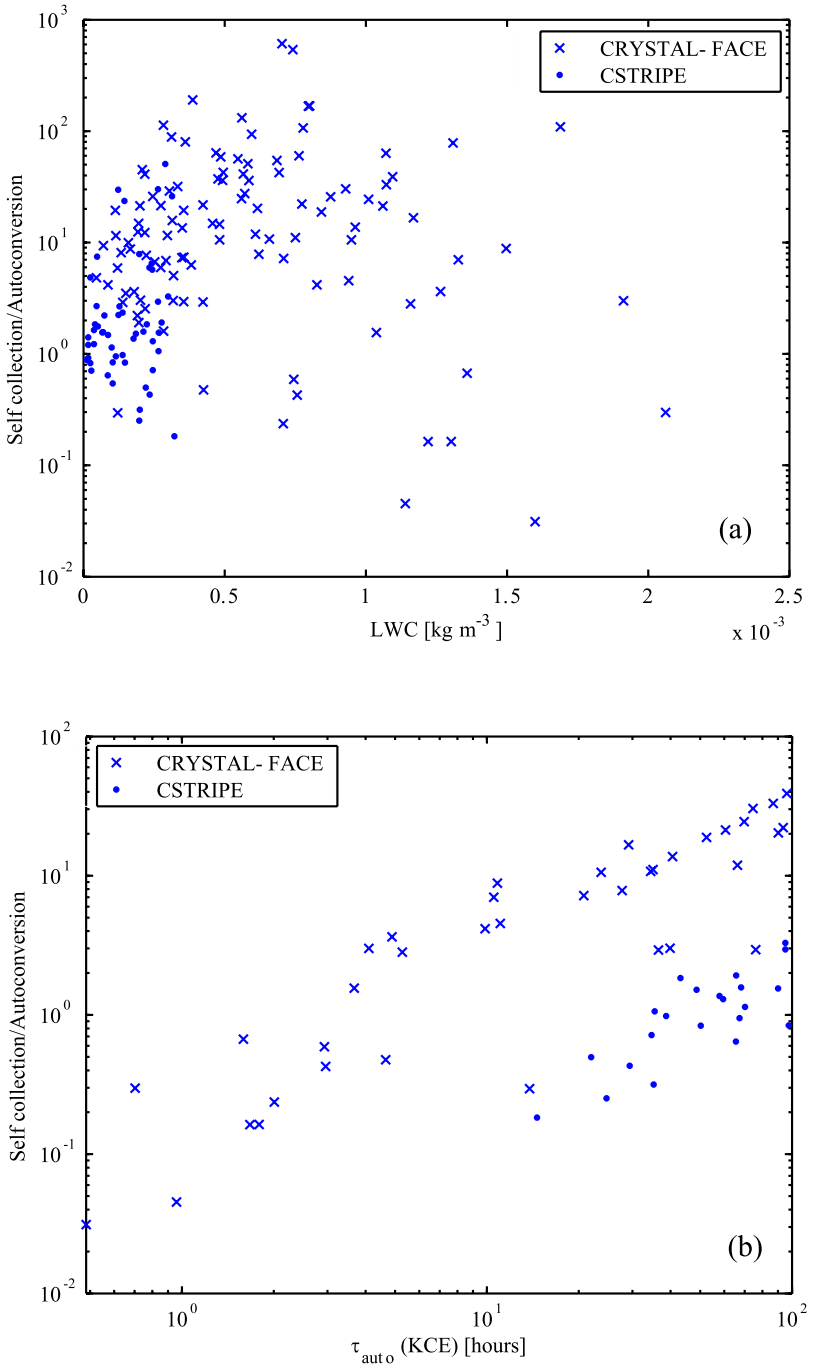

Figure 5. The ratio of self-collection to autoconversion versus (a) LWC and (b) τ_{auto} for CRYSTAL-FACE and CSTRIPE clouds.

uncertainty of the parameterization (~1–2 orders of magnitude [*Khairoutdinov and Kogan*, 2000]). A sensitivity analysis (section 4.3) suggests that the different thresholds used for KCE are not responsible for the bias and scatter of Figure 4. The other parameterizations in Table 2 do not give better results than KK. LD4 and MC closely agree with each other (Figures 4a and 4b) but substantially overestimate autoconversion, largely because both assume that the collection efficiency is independent of drop size [*Manton and Cotton*, 1977]. SD-L substantially overestimates as well, while SD-O agrees within a factor of 2 at high autoconversion rates. Large discrepancy between KCE calculations and parameterizations is also seen for the CSTRIPE DSDs (Figure 4b, Table 4); LD6 on average most closely approximates overall KCE calculations.

4.1. LD6 With Threshold Function

[21] The overestimation of autoconversion from LD6 was initially pointed out in the study of *Wood and Blossey* [2005]; in response, *Liu and Daum* [2005] state that LD6, which is a rate function, should be multiplied with a threshold function to give the autoconversion rate. In this

Table 4. Mean (Standard Deviation) of $\log(A_{KCE}/A_{param})$ and $\log(\tau_{KCE}/\tau_{param})$[a]

Parameterization	log (A_{KCE}/A_{param})	log $(\tau_{KCE}/\tau_{param})$
	CRYSTAL-FACE	
KK	1.43 (1.70)	−4.30 (1.67)
LD6	−2.75 (1.52)	0.79 (1.00)
LD6(T)	−1.89 (1.88)	0.66 (1.13)
LD4	−4.95 (1.74)	1.93 (0.79)
MC	−4.67 (1.80)	1.50 (0.82)
BH	2.81 (2.87)	−2.13 (2.18)
SD-O	−2.51 (2.30)	−0.39 (0.80)
SD-L	−0.66 (2.41)	−0.97 (0.99)
	CSTRIPE	
KK	3.34 (1.29)	−4.00 (0.80)
LD6	−0.50 (1.34)	0.18 (0.74)
LD6(T)	5.27 (3.96)	−5.85 (4.50)
LD4	−3.23 (1.33)	2.59 (0.58)
MC	−2.81 (1.40)	2.18 (0.62)
BH	6.46 (1.97)	−6.01 (1.49)
SD-O	2.05 (3.29)	−1.13 (1.44)
SD-L	4.80 (3.30)	−3.88 (1.46)

[a]Error statistics for LD6 multiplied with the threshold function (T), parameterization are computed for data points with an autoconversion rate > 10^{-9} kg m^{-3} s^{-1}.

section, we evaluate LD6 multiplied by the autoconversion threshold function, T_ε, of *Liu et al.* [2006],

$$T_\varepsilon = \gamma'\left(\frac{6+\varepsilon^{-1}}{\varepsilon^{-1}}, \gamma^{1/(3\varepsilon)}\left(\frac{3+\varepsilon^{-1}}{\varepsilon^{-1}}\right)x_c^{1/(3\varepsilon)}\right) \cdot \gamma'\left(\frac{3+\varepsilon^{-1}}{\varepsilon^{-1}}, \gamma^{1/(3\varepsilon)}\left(\frac{3+\varepsilon^{-1}}{\varepsilon^{-1}}\right)x_c^{1/(3\varepsilon)}\right) \quad (12)$$

where x_c is the critical-to-mean mass ratio, and $\gamma' = \gamma/\Gamma$.

[22] Figure 6 shows the generalized threshold function as a function of the mean-to-critical mass ratio (x_c^{-1}), for DSDs of constant ε (lines), CRYSTAL-FACE (dots) and CSTRIPE clouds (circles). The threshold function values are close to the theory for $\varepsilon = 0.36$ for many cases of CRYSTAL-FACE clouds; the computed threshold function for CSTRIPE DSDs is less than 0.3, very often with values less than 10^{-1}. This suggests that such clouds are far away from a precipitating state, and is consistent with the timescale analysis of section 5. Figure 7 presents predictions of autoconversion using LD6 (with and without the threshold function) against the KCE computations. Considering the threshold function decreases the autoconversion rate (mostly for the CSTRIPE clouds furthest away from a precipitating state), but the changes are not significant in high autoconversion rates for CRYSTAL-FACE (since the value of the threshold function is close to unity). The reduction of autoconversion using the threshold function is sometimes large enough to result in an underestimation of autoconversion, especially for CSTRIPE clouds.

4.2. Accuracy of Long's Approximate Polynomial

[23] It is important to quantify the uncertainty introduced in calculated coalescence (and autoconversion) rate from using the polynomial approximation to Long's gravitational collection kernel. This is shown in Figure 8, which presents total coalescence (Figure 8, top) and autoconversion rate (Figure 8, bottom) calculations using explicit gravitational collection and approximate polynomial kernels, for CRYSTAL-FACE DSDs. On average, using Long's approximate polynomial overestimates total coalescence rate by up to a factor of 13, and 32% for autoconversion. These deviations are most prominent at low conversion rates, while the agreement at higher values (most relevant for precipitation) is quite good.

4.3. Effect of Drizzle Threshold Size, r_0

[24] The large discrepancy of autoconversion rate between parameterizations may in part be from the separating

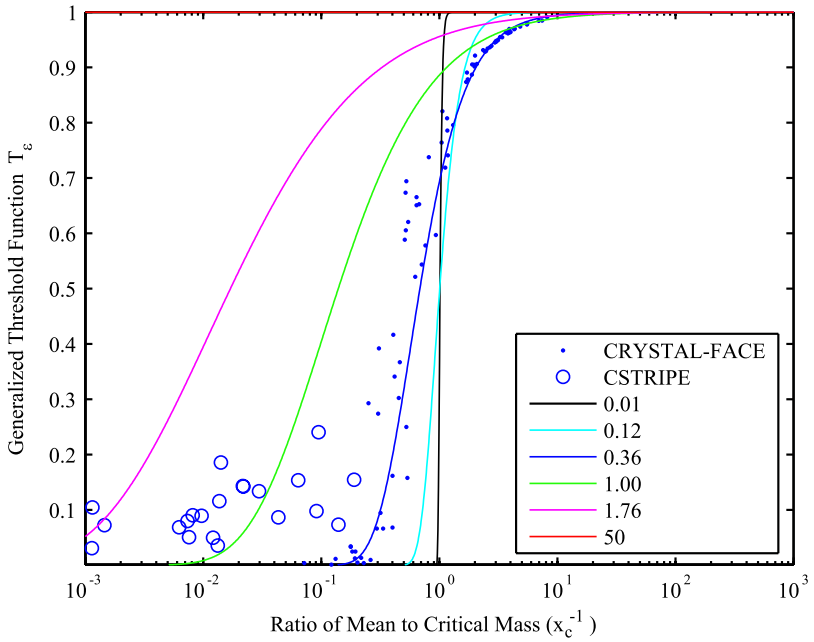

Figure 6. The generalized threshold function by *Liu et al.* [2006]. Lines represent the threshold function for constant ε (values given in legend). Circles and dots represent CRYSTAL-FACE and CSTRIPE DSDs, respectively.

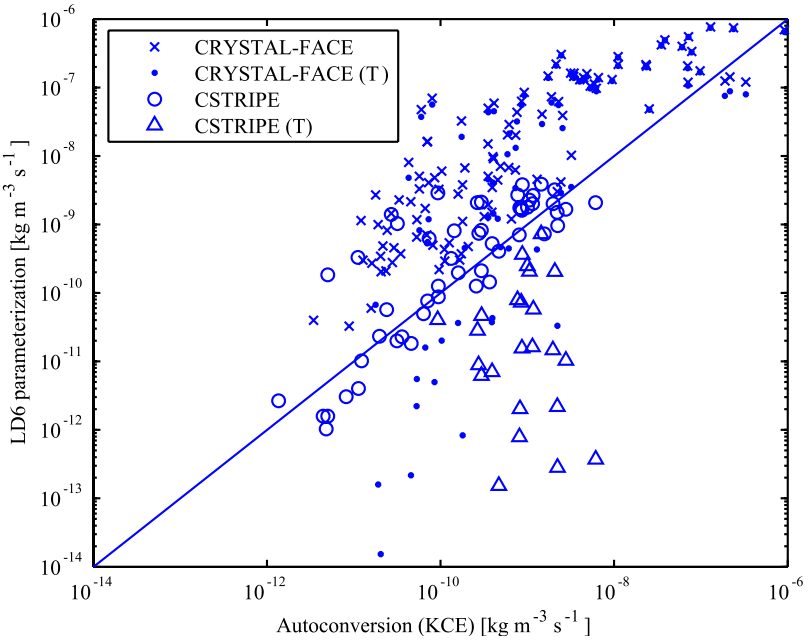

Figure 7. Comparison of autoconversion rate (kg m^{-3} s^{-1}) between LD6 parameterization and KCE integration for CRYSTAL-FACE and CSTRIPE DSD. (T) in legends denotes the consideration of threshold function when applying LD6 scheme.

size used to distinguish cloud droplets from drizzle drops. In this section, we analyze the effects of changing r_0 from 20 μm (as suggested by *Wood and Blossey* [2005]) to 25 μm [*Khairoutdinov and Kogan*, 2000] for DSDs observed in CRYSTAL-FACE clouds. The calculations were done based on Long's gravitational collection kernel, the results of which are summarized in the first two columns of Table 5. As compared to the calculation with $r_0 = 20$ μm, the relative difference of autoconversion rate could increase to 235% when $r_0 = 25$ μm is used. In general, lower autoconversion rates are obtained for $r_0 = 25$ μm but a slightly higher value for coalescence (Figure 9). The relative difference for autoconversion rate is up to −86% and 11% for total coalescence (Table 5). Compared to coalescence, changes in autoconversion are subject to significantly more scatter (Figure 9), suggesting that the effect of r_0 on collection may not be monotonic.

5. Autoconversion Error for Hydrologically Sensitive Clouds

[25] Autoconversion rates vary over five orders of magnitude in the CRYSTAL-FACE and four orders of magnitude for CSTRIPE data sets. Not all of this dynamic range is "hydrologically important" (as noted in section 2.2) so we focus the evaluation for clouds closest to forming drizzle. The evaluation is done by computing τ_{auto} for each observed DSD, using the parameterized and KCE-computed values of autoconversion. Results of this intercomparison for CRYSTAL-FACE and CSTRIPE clouds are shown in Figures 10a and 10b, respectively. τ_{auto} ranges from 0.5 to 10^4 h in cumulus (CRYSTAL-FACE) and 10 to 10^4 h for stratocumulus clouds (CSTRIPE). The CSTRIPE data tend to exhibit larger τ_{auto}, consistent with the lower LWC, weaker dynamical forcing, and low cloud top height. In this study, the "hydrologically important" clouds are those with τ_{auto} less than the typical cloud lifetime, multiplied by a factor of ten to account for the order of magnitude uncertainty associated with autoconversion parameterizations. Thus, for CRYSTAL-FACE clouds, τ_{auto} ranges between 0.1 and 10 h; for CSTRIPE data, τ_{auto} ranges between 0.1 and 100 h. Compared with KCE, application of LD6 tends to underestimate τ_{auto} (because autoconversion rate is overestimated) and they differ by a factor of about 0.79 ± 1.00 for CRYSTAL-FACE and 0.18 ± 0.74 for CSTRIPE clouds (Table 4). In terms of the other parameterizations, the difference is larger than a factor of 2 for KK and BH in CRYSTAL-FACE clouds and KK, LD4, MC, BH, and SD-L for CSTRIPE cases. LD6 with threshold function, LD6(T), has the lowest error in τ_{auto} and this is consistent with its good agreement in autoconversion rate (Table 4). Among the formulations applied, the standard deviation of A (or τ_{rain}), is of order of the error in τ_{rain} (Table 4). Given that was seen in all parameterizations studied, regardless of their sophistication, this finding may suggest that "tuning" of parameterizations to minimize the average τ_{rain} error (instead of A or LWC), may be accompanied by a strong reduction in prediction scatter, and be an efficient way to improve autoconversion predictions in GCMs.

6. KCE With Turbulent Kernel

[26] LD6 and other parameterizations have been derived assuming that gravitational setting under "quiescent flow" conditions govern droplet collision. However, it is well known that turbulence can affect droplet growth and enhance collision coalescence process [*Pruppacher and Klett*, 1997; *Xue et al.*, 2008]. We compare autoconversion rates using KCE with a gravitational kernel, and KCE with a kernel enhanced by turbulent coalescence. In this study, the effect of turbulence on the droplet collection process is

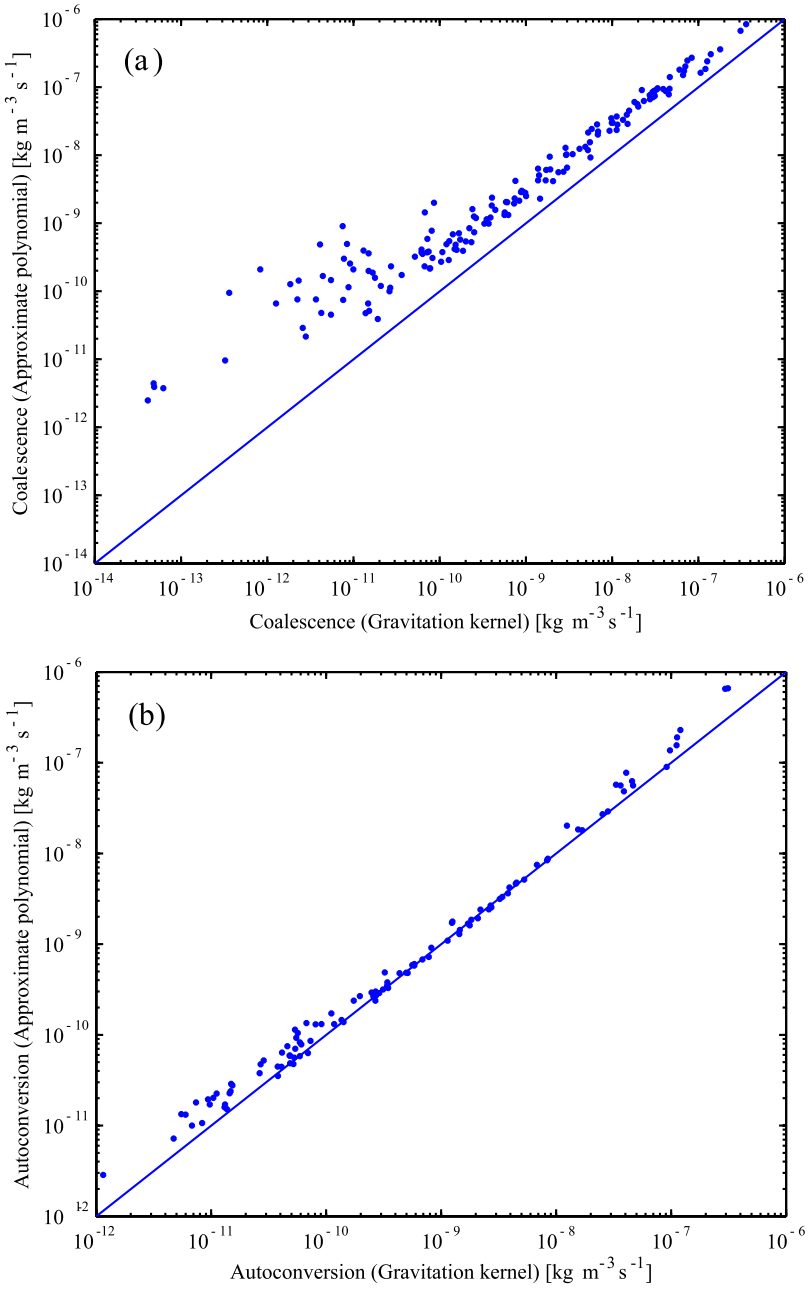

Figure 8. Comparison of (a) total coalescence and (b) autoconversion rate between polynomial approximation and explicit gravitational collection kernel for CRYSTAL-FACE DSDs.

represented by application of two collection kernels, by (1) *Zhou et al.* [2001] and (2) *Ayala et al.* [2008a, 2008b]. Both kernels are derived from direct numerical simulation (DNS) of droplet collection in a turbulent field. The parameterizations of the turbulent collision kernel presented in these studies make use of a general turbulent velocity correlation function, thus partially removing the low Reynolds number limitation in DNS. *Xue et al.* [2008] showed that the kernel of *Zhou et al.* [2001] severely overestimate the effects of turbulence at the very high Reynolds number expected in ambient clouds; nevertheless, we include it in our assessment, to serve as an upper limit of the effect of turbulence on droplet collection.

6.1. Turbulence Kernel by *Zhou et al.* [2001]

[27] The collection kernel is of the form:

$$K_t(r_1, r_2) = E_t \Gamma_0 \left[1 + 15 \frac{w_r^2}{v_k^2} \left(\frac{\eta}{R}\right)^2\right]^{1/2} g_{12}(R) \qquad (13)$$

where $R = r_1 + r_2$, $\Gamma_0 = (8\pi/15)^{1/2} R^3 v_k(R/\eta)$, $g_{12}(R)$ is given by *Zhou et al.* [2001], and, r_1, r_2 are radii of the droplets involved in the collision. $v_k = (\nu e)^{1/4}$ is the Kolmogorov velocity scale, ν is the kinematic viscosity of the fluid and e is the turbulent dissipation rate. $\eta = (\nu^3/e)^{1/4}$ is the Kolmogorov length scale, and, E_t is the turbulent collection efficiency (assumed to be unity) [*Riemer and Wexler*, 2005].

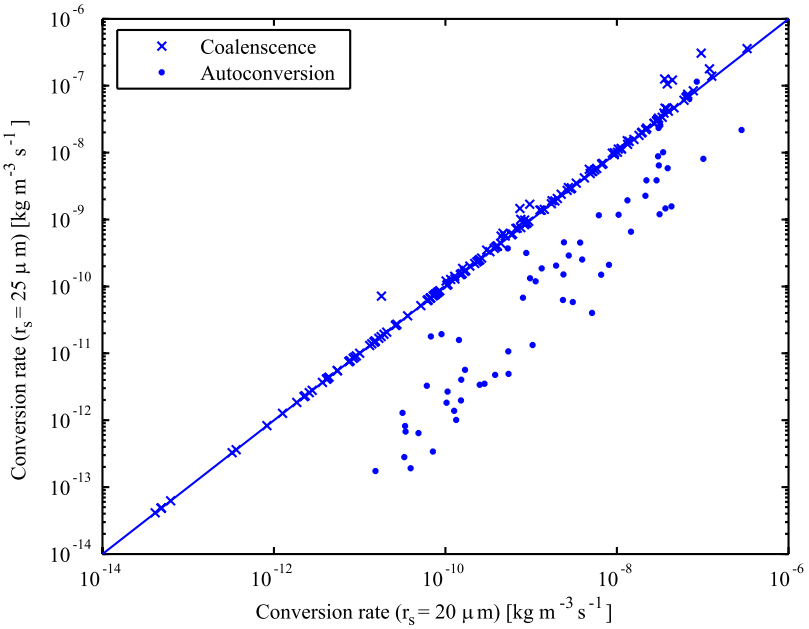

Figure 9. Comparison of conversion rate (total coalescence and autoconversion) between $r_0 = 25$ μm and $r_0 = 20$ μm for CRYSTAL-FACE DSDs.

Also,

$$\frac{w_r^2}{v_k^2} = C_w(\phi)\left(\frac{u'}{v_k}\right)^2 \frac{\gamma}{\gamma - 1}\left\{(\theta_1 + \theta_2) - \frac{4\theta_1\theta_2}{\theta_1 + \theta_2}\left[\frac{1 + \theta_1 + \theta_2}{(1 + \theta_1)(1 + \theta_2)}\right]^{\frac{1}{2}}\right\} \cdot \left\{\frac{1}{(1 + \theta_1)(1 + \theta_2)} - \frac{1}{(1 + \gamma\theta_1)(1 + \gamma\theta_2)}\right\} \quad (14)$$

where $\theta_i = \frac{2.5\tau_{pi}e}{u'^2}$, i (= 1, 2) is the index for droplets involved in the collection, and, u' is the root mean square velocity fluctuation in the flow. $C_w(\phi)$, γ and ϕ are given by *Zhou et al.* [2001]. $\tau_{pi} = 2\rho_i r_i^2/(9\nu\rho)$ is the droplet inertial response time, and ρ_i, ρ is the particle and air density, respectively.

[28] Equation (13) is developed in the absence of gravitational collection. To compute collection rates in the presence of both gravity and turbulence, we add equation (13) to the gravitational kernel of *Long* [1974].

6.2. Turbulence Kernel by *Ayala et al.* [2008a, 2008b]

[29] The kernel of *Ayala et al.* [2008a, 2008b] considers simultaneously the effects of gravity and turbulence on collection,

$$K_t(r_1, r_2) = 2\pi R^2 \langle |w_r(R)| \rangle g_{12}(R) E_{12}^g \quad (15)$$

where $\langle |w_r| \rangle$ is the radial relative velocity and E_{12}^g is the collision efficiency of droplets with radii r_1, r_2 in a quiescent background air. The radial distribution function at contact, $g_{12}(R)$, is given by *Ayala et al.* [2008a, 2008b]. The effects of turbulence on geometric collision kernel is considered; turbulent effects on collision efficiency is not included because efficiency data is not available for the dissipation rates relevant for ambient clouds. Gravitational collection efficiency is obtained from the Hall kernel, and, terminal velocities of droplets are determined by the nonlinear drag. $\langle |w_r| \rangle$ is expressed as [*Ayala et al.*, 2008a, 2008b],

$$\langle |w_r| \rangle = \sqrt{\frac{2}{\pi}}\sigma\left[\frac{1}{2}\sqrt{\pi}\left(b + \frac{0.5}{b}\right) erf(b) + \frac{1}{2}\exp(-b^2)\right] \quad (16)$$

The variance of the relative velocity fluctuation, σ^2, is given as

$$\sigma^2 = \left\langle (v_1')^2 \right\rangle + \left\langle (v_2')^2 \right\rangle - 2\langle (v_1' v_2') \rangle \quad (17)$$

where v'_1 and v'_2 are the fluctuational velocity of two colliding droplets in the radial direction. Finally, the parameter b is defined as

$$b = \frac{|v_{t,1} - v_{t,2}|}{\sigma\sqrt{2}} \quad (18)$$

where $v_{t,1}$ and $v_{t,2}$ are the terminal velocity of droplets with radius r_1 and r_2, respectively.

6.3. Effects of Turbulence on Collection

[30] K_t requires knowledge of the fluctuational velocity, u', and dissipation rate, e (which express the intensity of the

Table 5. Difference in KCE Conversion Rates Using the Polynomial and Gravitational Collection Kernel, Relative to the Gravitational Kernel[a]

Conversion Rate	$r_0 = 20$ μm	$r_0 = 25$ μm	Relative Difference
Total coalescence	12.33	12.21	0.11
Autoconversion	0.32	2.35	−0.86
Self-collection	13.14	12.18	0.76

[a]Results are shown for $r_0 = 20$ μm and $r_0 = 25$ μm. Also shown is relative difference in conversion rate (using the explicit gravitational kernel) between $r_0 = 25$ μm and $r_0 = 20$ μm, with respect to $r_0 = 20$ μm.

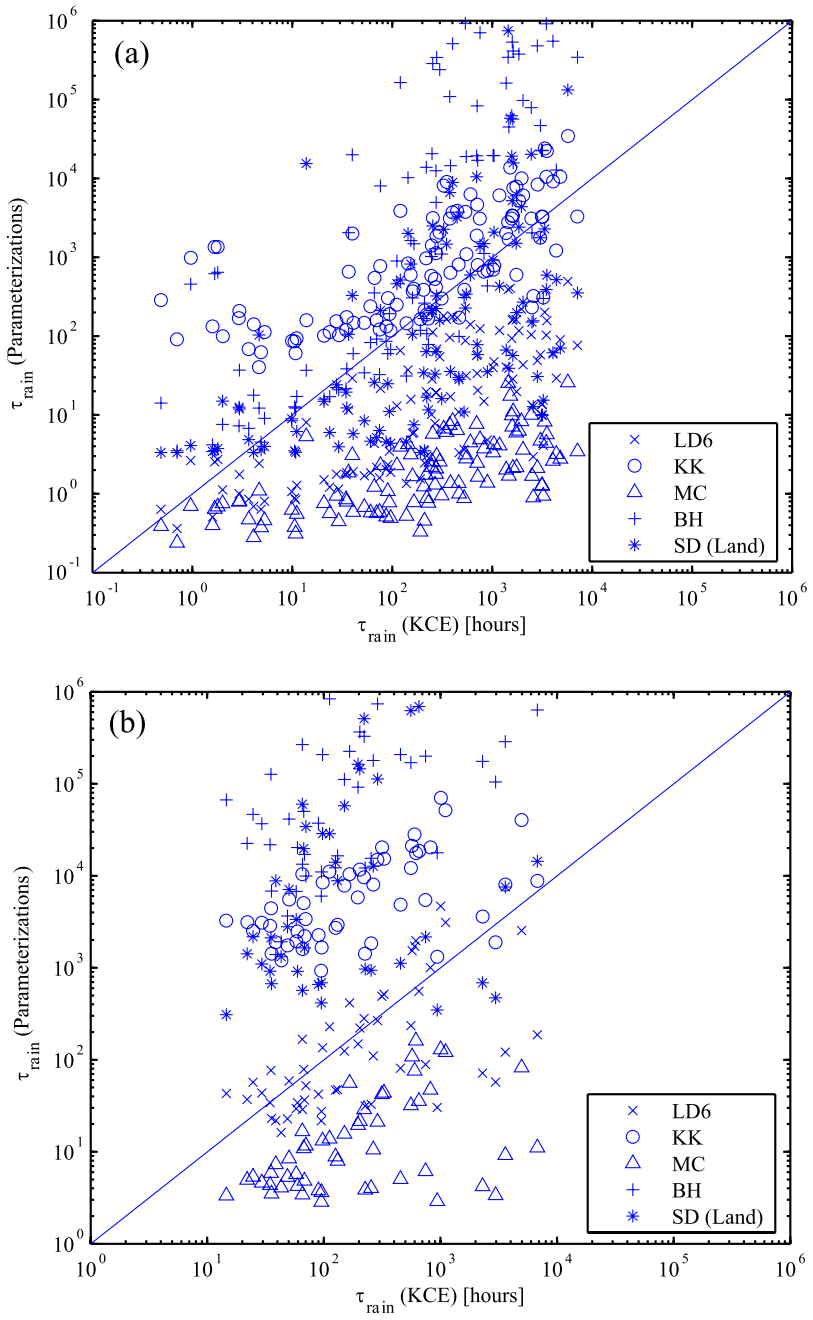

Figure 10. τ_{auto} (Parameterizations) versus τ_{auto} (KCE) for (a) CRYSTAL-FACE and (b) CSTRIPE clouds.

turbulent field surrounding the droplet population). In general, e varies from tens cm^2 s^{-3} for stratus clouds to several hundreds cm^2 s^{-3} for cumuli [*Pruppacher and Klett*, 1997]. Therefore e = 200 cm^2 s^{-3} for CRYSTAL-FACE clouds, and, e = 50 cm^2 s^{-3} for CSTRIPE clouds are assumed; u' can then be inferred from e using the u' vs. e correlation from studies of *MacPherson and Isaac* [1977] and *Riemer and Wexler* [2005]. As pointed out by *Wang et al.* [2006], *Riemer and Wexler* [2005] overestimates u' by a factor of $\sqrt{3}$, thus a correction of this factor is also included. The average u' used for CRYSTAL-FACE clouds is thus 1.73 m s^{-1} and 1.15 m s^{-1} for CSTRIPE clouds.

[31] Figure 11 compares autoconversion rates obtained from KCE integration with gravitational collection under quiescent and turbulent conditions. The Hall kernel is used for gravitational collision process since the kernel by *Ayala et al.* [2008a, 2008b] is based on the setting of still-fluid terminal velocity and collision efficiency of Hall kernel. Both kernels by *Ayala et al.* [2008a, 2008b] and *Zhou et al.* [2001] are included. For CRYSTAL-FACE cloud size distributions, the average autoconversion rate augmented by the kernel of *Ayala et al.* [2008a, 2008b] is about a factor of 1.82 ± 0.09 greater than the average value obtained using the gravitational kernel alone. When applied to CSTRIPE clouds, turbulence enhances autoconversion by a factor of

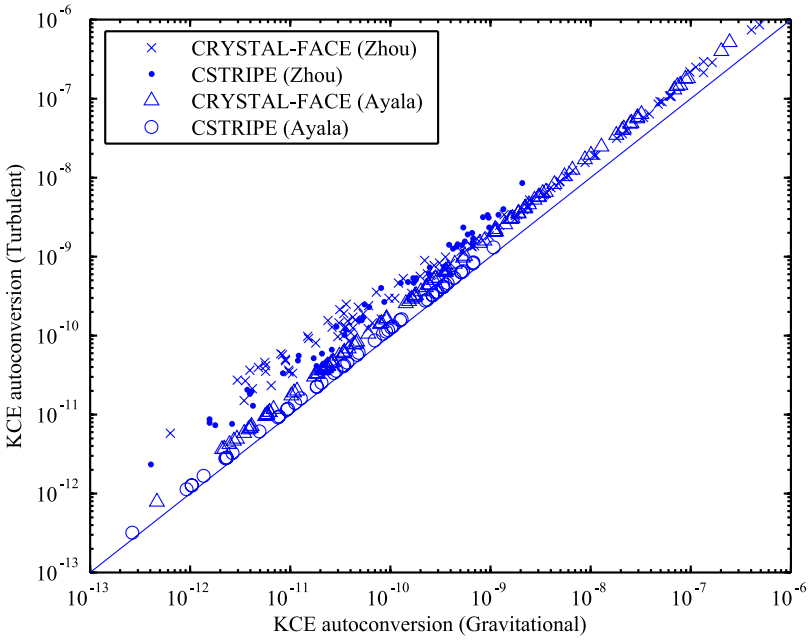

Figure 11. KCE autoconversion rates (kg m^{-3} s^{-1}) using turbulent and quiescent conditions, for CRYSTAL-FACE and CSTRIPE DSD.

1.24 ± 0.01; this difference may be important for clouds for which the time needed for initializing precipitation is slightly longer than its lifetime. When the turbulence kernel of *Zhou et al.* [2001] is added to the gravitational kernel, average autoconversion rate increases (compared with a calculation using the gravitational kernel only) by a factor of 3.3 ± 2.0 for CRYSTAL-FACE clouds, and 3.5 ± 0.9 for CSTRIPE clouds. Thus, though the kernel of *Zhou et al.* [2001] severely overestimates the turbulent kernel [*Xue et al.*, 2008] and predicts higher autoconversion for the less dissipating CSTRIPE clouds, the effect on autoconversion is about a factor of two different from using the more atmospherically relevant kernel of *Ayala et al.* [2008a, 2008b]. For the hydrologically important clouds in the data set, turbulence (using the kernel of *Ayala et al.* [2008a, 2008b]) enhances autoconversion on average by 96% for CRYSTAL-FACE and 24% for CSTRIPE clouds. Although important, the effect of turbulence tends to lie within the inherent uncertainty of autoconversion parameterizations.

7. Computational Requirements of KCE

[32] Assuming that the parameterization-KCE autoconversion discrepancy is representative of the parameterization (process) error, one can use KCE as a benchmark calculation. Although expensive for usage in a GCM simulation, KCE can be substantially accelerated if precalculated lookup tables are used for $K(r_1, r_2)$, in place of an online calculation. To evaluate the potential speedup and the impact of using discretized kernels on the calculation, we compare A predicted from KCE (with a lookup table where droplet radii range from 1 to 100 μm with an increment of 1 μm) vs. A from KCE with online calculation of collection kernels. The time needed for computing A from KCE integration is then evaluated for all CRYSTAL-FACE clouds (a total of 164 spectra). Each KCE calculation is executed for all DSDs from CRYSTAL-FACE, and the average time per computation is compared against that required for LD6; the computational platform used for the intercomparison was done in Matlab run on an Intel Pentium-4 2.40 GHz PC running the Windows XP operating system. The total execution time for computing A with KCE calculation includes the procedure of fitting the size distributions and the discretization of the resulting droplet distribution into the droplet bins. Table 6 displays the CPU times of all calculations; KCE integration with a lookup table for kernels is $\sim$2.4 times slower than LD6. Including threshold function for LD6 has the effect to increase computation time, but to a small extent. On average, LD6 with threshold function included is about a factor of 1.07 slower than LD6, but a factor of $\sim$2.2 faster than KCE integration. This suggests that application of KCE may be computationally feasible in large-scale models, at least for studies that explicitly resolve cloud droplet spectra. Prescribing ε and obtaining N and LWC from an online simulation may further speedup LD6 by a factor of 2.

8. Conclusions

[33] This study evaluates assumptions used in autoconversion parameterization development, by comparing them against predictions of the KCE applied to ambient cloud droplet size distributions collected during the CRYSTAL-FACE and CSTRIPE field campaigns. First, the P6 parameterization of *Liu and Daum* [2004] is compared against KCE calculations for gamma distribution fits to the ambient data; both are in excellent agreement for total coalescence. This agreement is largely preserved even when the ambient droplet distribution data is used in the KCE calculation. This means that a gamma distribution provides a good approximation to ambient distributions for calculations of total coalescence, and, the polynomial collection kernel

Table 6. CPU Time Required for Computing Autoconversion Using LD6 (Only Rate Function and Both Rate and Threshold Function Considered) and KCE Integration With Lookup Tables for Collection Kernel

	CPU Time (s)	
Calculation Method	All Executions (164)	Average
KCE (pre-process kernel)	5.89	3.59×10^{-2}
LD6	2.48	1.51×10^{-2}
LD6 (with threshold function)	2.66	1.62×10^{-2}

(used in the analytical integration of the KCE) is a good approximation to the full formulation.

[34] The error in autconversion from fitting a gamma distribution to the data is also assessed. This is done by comparing KCE calculations of autoconversion, using the observed droplet distributions vs. their gamma distribution fits. The error from the fitting is much greater than for total coalescence and most of this uncertainty arises from the deviations in the fitted distribution, especially for droplet sizes that are close to the drizzle-drop separation threshold. This suggests that higher moments of the DSD (like skewness) may need to be accounted for an effective parameterization of the autoconversion process, in a way so that errors in the fitted distribution are minimized in the region near the drizzle-drop separation size.

[35] KCE calculations of autoconversion rate are also compared against parameterizations currently used in models. Of all parameterizations that consider droplet number, the formulation of *Khairoutdinov and Kogan* [2000] on average gives the lowest error and scatter for CRYSTAL-FACE clouds, the latter of which is still substantial ($\sim$1 order of magnitude). When the parameterizations are used to predict autoconversion timescale, τ_{auto}, LD6 has the lowest average error. Multiplying LD6 with a threshold function has a minor impact on predicted autoconversion rate for CRYSTAL-FACE clouds, and, a major impact on CSTRIPE clouds. This is consistent with timescale analysis that most of CSTRIPE clouds are far from precipitating state. For higher autoconversion rates in CRYSTAL-FACE clouds, the threshold function is close to unity, consistent with the small autoconversion timescale associated with these clouds.

[36] We also explore the sensitivity of predicted autoconversion to the droplet size threshold used for separating cloud droplets from drizzle. Varying r_0 from 20 to 25 μm radius affects autoconversion to within a factor of two, and the predicted autoconversion rates tend to be lower when using 25 μm. Overall, the autoconversion difference rising from ambiguity in r_0 is considerably smaller than the inherent scatter of all parameterizations examined.

[37] We also assess the importance of including turbulence effect in KCE calculations of autoconversion rate. Neglecting the turbulent collection process can introduce systematic biases in autoconversion calculations, as enhancement from turbulence is on average by a factor of 1.82 in CRYSTAL-FACE, and, 1.24 in CSTRIPE clouds using the most realistic kernel of *Ayala et al.* [2008a, 2008b]. This difference, although within the inherent uncertainty of autoconversion parameterizations, may be important for clouds close to forming precipitation. Surprisingly, collection enhancement from turbulence may be less sensitive to the kernel used as previously thought. Using the kernel of *Zhou et al.* [2001], which is known to substantially overestimate turbulence collection for conditions found in clouds, enhances autoconversion rate by roughly a factor of 3 and can be considered an upper limit in enhancement from turbulence.

[38] Finally, we evaluate the computational efficiency of KCE against autoconversion parameterizations. We find that using lookup tables, in place of online calculation of collection kernels result in a considerable acceleration of KCE calculations, which become roughly 2.5–4 times slower than application of the LD6 parameterization. This, together with the substantial predictive uncertainty of current autoconversion parameterizations, suggests that direct KCE integration could be included in studies of the aerosol indirect effect.

[39] **Acknowledgments.** Support was provided by the Department of Energy, an NSF CAREER award, the Office of Naval Research under grant N00014-04-1-0118, and the School of Earth and Atmospheric Science at Georgia Institute of Technology. We thank Dr. Andreas Bott for sharing his KCE code and Dr. Yangang Liu for helpful discussions. Finally, we thank three anonymous reviewers for their constructive comments. W.C.H. thanks Chien-Yu Peng for assistance in numerical techniques.

References

Abramowitz, M., and I. Stegun (1965), *Handbook of Mathematical Functions*, Dover, New York.

Albrecht, B. A. (1989), Aerosols, cloud microphysics, and fractional cloudiness, *Science*, *245*, 1227–1230.

Ayala, O., B. Rosa, L.-P. Wang, and W. W. Grabowski (2008a), Effects of turbulence on the geometric collision rate of sedimenting droplets: part 1. Results from direct numerical simulation, *New J. Phys.*, *10*, 075,015.

Ayala, O., B. Rosa, L.-P. Wang, and W. W. Grabowski (2008b), Effects of turbulence on the geometric collision rate of sedimenting droplets: part 2. Theory and parameterization, *New J. Phys.*, *10*, 075,016.

Baker, M. B. (1993), Variability in the concentrations of cloud condensations nuclei in the marine cloud-topped boundary layer, *Tellus*, *45B*, 458–472.

Baumgardner, D., H. Jonsson, W. Dawson, D. O'Connor, and R. Newton (2001), Cloud, aerosol and precipitation spectrometer: A new instrument for cloud investigations, *Atmos. Res.*, *59–60*, 251–264.

Beheng, K. D. (1994), A parameterization of warm cloud microphysical conversion processes, *Atmos. Res.*, *33*, 193–206.

Beheng, K. D., and G. Doms (1986), A general formulation of collection rates of cloud and raindrops using the kinetic equation and comparison with parameterizations, *Beitr. Phys. Atmos.*, *59*, 66–84.

Brenguier, J.-L., T. Bourrianne, A. Coelho, J. Isbert, R. Peytavi, D. Trevarin, and P. Weschler (1998), Improvements of droplet size distribution measurements with the fast-FSSP (forward scattering spectrometer probe), *J. Atmos. Ocean. Tech.*, *15*, 1077–1090.

Cohard, J., and J. Pinty (2000), A comprehensive two-moment warm microphysical bulk scheme. I: Description and tests, *Q. J. R. Meteorol. Soc.*, *126*, 1815–1842.

Conant, W., et al. (2004), Aerosol-cloud drop concentration closure in warm cumulus, *J. Geophys. Res.*, *109*, D13204, doi:10.1029/2003JD004324.

Del Genio, A. D., M.-S. Yao, W. Kovari, and K.-W. Lo (1996), A prognostic cloud water parameterization for global climate models, *J. Clim.*, *9*, 270–304.

Intergovernmental Panel on Climate Change (IPCC) (2007), *Climate Change 2007: The Physical Science Basis*, Cambridge Univ. Press, U. K.

Jones, A., D. L. Roberts, and M. J. Woodage (2001), Indirect sulphate aerosol forcing in a climatic model with an interactive sulphur cycle, *J. Geophys. Res.*, *106*, 20,293–30,310.

Kessler, E. (1969), On the distribution and continuity of water substance in atmospheric circulation, *Meteorol. Monogr. 32*, 84 pp., Am. Meteorol. Soc., Boston, Mass.

Khairoutdinov, M., and Y. Kogan (2000), A new cloud physics parameterization in a large-eddy simulation model of marine stratocumulus, *Mon. Weather Rev.*, *128*, 229–243.

Liu, Y., and P. H. Daum (2004), Parameterization of the autoconversion process. part I: Analytical formulation of the Kessler-type parameterizations, *J. Atmos. Sci.*, *61*, 1539–1548.

Liu, Y., and P. H. Daum (2005), Reply, *J. Atmos. Sci.*, *62*, 3007–3008.

Liu, Y., P. H. Daum, R. McGraw, and M. Miller (2006), Generalized threshold function accounting for effect of relative dispersion on threshold behavior of autoconversion process, *Geophys. Res. Lett.*, *33*, L11804, doi:10.1029/2005GL025500.

Lohmann, U., and J. Feichter (1997), Impact of sulfate aerosols on albedo and lifetime of clouds: A sensitivity study with the ECHAM4 GCM, *J. Geophys. Res.*, *102*, 13,685–13,700.

Lohmann, U., and J. Feichter (2005), Global indirect aerosol effects: A review, *Atmos. Chem. Phys.*, *5*, 715–737.

Long, A. B. (1974), Solutions to droplet collection equation for polynomial kernels, *J. Atmos. Sci.*, *31*, 1040–1052.

MacPherson, J. I., and G. A. Isaac (1977), Turbulence characteristics of some Canadian cumulus clouds, *J. Appl. Meteorol.*, *16*, 81–90.

Manton, M. J., and W. R. Cotton (1977), Formulation of approximate equations for modeling moist deep convection on the mesoscale, *Atmos. Sci. Pap. 266*, 62 pp., Colorado State Univ., Fort Collins, Colo.

Menon, S., A. D. Del Genio, D. Koch, and G. Tselioudis (2002), GCM simulations of the aerosol indirect effect: Sensitivity to cloud parameterization and aerosol burden, *J. Atmos. Sci.*, *59*, 692–713.

Menon, S., et al. (2003), Evaluating aerosol/cloud/radiation process parameterizations with single-column models and Second Aerosol Characterization Experiment (ACE-2) cloudy column observations, *J. Geophys. Res.*, *108*(D24), 4762, doi:10.1029/2003JD003902.

Meskhidze, N., A. Nenes, W. C. Conant, and J. H. Seinfeld (2005), Evaluation of a new cloud droplet activation parameterization with in situ data from CRYSTAL-FACE and CSTRIPE, *J. Geophys. Res.*, *110*, D16202, doi:10.1029/2004JD005703.

Pruppacher, H. R., and J. D. Klett (1997), *Microphysics of Clouds and Precipitation*, Springer, Norwell, Mass.

Randall, D., M. Khairoutdinov, A. Arakawa, and W. Grabowski (2003), Breaking the cloud parameterization deadlock, *Bull. Am. Meteorol. Soc.*, *84*, 1547–1564.

Riemer, N., and A. S. Wexler (2005), Droplets to drops by turbulent coagulation, *J. Atmos. Sci.*, *62*, 1962–1975.

Riemer, N., A. S. Wexler, and K. Diehl (2007), Droplet growth by gravitational coagulation enhanced by turbulence: Comparison of theory and measurements, *J. Geophys. Res.*, *112*, D07204, doi:10.1029/2006JD007702.

Rotstayn, L. D. (1997), A physically based scheme for the treatment of stratiform clouds and precipitation in large-scale models. I: Description and evaluation of the microphysical processes, *Q. J. R. Meteorol. Soc.*, *123*, 1227–1282.

Seifert, A., and K. D. Beheng (2001), A double-moment parameterization for simulating autoconversion, accretion and self collection, *Atmos. Res.*, *59–60*, 265–281.

Sundqvist, H., E. Berge, and J. E. Kristjansson (1989), Condensation and cloud parameterization studies with a mesoscale numerical weather prediction model, *Mon. Weather Rev.*, *117*, 1641–1657.

Twomey, S. (1977), The influence of pollution on the shortwave albedo of clouds, *J. Atmos. Sci.*, *34*, 1149–1152.

VanReken, T. M., T. A. Rissman, G. C. Roberts, V. Varutbangkul, H. H. Jonsson, R. C. Flagan, and J. H. Seinfeld (2003), Toward aerosol/cloud condensation nuclei (CCN) closure during CRYSTAL-FACE, *J. Geophys. Res.*, *108*(D20), 4633, doi:10.1029/2003JD003582.

Wang, L. P., O. Ayala, Y. Xue, and W. W. Grabowski (2006), Comments on "Droplets to drops by turbulent coagulation", *J. Atmos. Sci.*, *63*, 2397–2401.

Wood, R. (2005), Drizzle in stratiform boundary layer clouds. part II: Microphysical aspects, *J. Atmos. Sci.*, *62*, 3034–3050.

Wood, R., and P. N. Blossey (2005), Comments on "Parameterization of the autoconversion process. part I: Analytical formulation of the Kessler-type parameterizations", *J. Atmos. Sci.*, *62*, 3003–3006.

Xue, Y., L.-P. Wang, and W. W. Grabowski (2008), Growth of cloud droplets by turbulent collision-coalescence, *J. Atmos. Sci.*, *65*, 331–356.

Zhou, Y., A. S. Wexler, and L.-P. Wang (2001), Modelling turbulent collision of bidisperse inertial particles, *J. Fluid Mech.*, *433*, 77–104.

G. Buzorius, Department of Meteorology, Graduate School of Engineering and Applied Sciences, Naval Postgraduate School, 1 University Circle, Monterey, CA 93943, USA.

R. C. Flagan and J. H. Seinfeld, Environmental Science and Engineering, California Institute of Technology, 1200 E. California Boulevard, Pasadena, CA 91125, USA.

W. C. Hsieh and A. Nenes, School of Earth and Atmospheric Sciences, Georgia Institute of Technology, 331 Ferst Drive, Atlanta, GA 30332-0340, USA. (nenes@eas.gatech.edu)

H. Jonsson, Center for Interdisciplinary Remotely-Piloted Aircraft Studies, 3200 Imjin Road, Marina, CA 93933, USA.

L.-P. Wang, Department of Mechanical Engineering, University of Delaware, 126 Spencer Laboratory, Newark, DE 19716-3140, USA.